AIAA Journal

VOLUME 9 JULY 1971 NUMBER 7

1970 Von Kármán Lecture

Physics of Turbulent Flow

ERIK MOLLO-CHRISTENSEN
Massachusetts Institute of Technology, Cambridge, Mass.

I. Introduction

THE intensive research by many investigators in the last twenty years has yielded many results and numerous bits and pieces of understanding of partial processes which occur in turbulence. A picture of turbulent flows now seems to be emerging which can guide further research and be directly practically useful at least in a qualitative sense. I shall attempt to describe elements of this picture in terms of the physics of partial processes and observations. What I have to say is not new and does not yield new quantitative results, but may be helpful in further work.

Turbulence is a random process. We cannot and do not want to know all the details of a random process. We have to limit ourselves to a knowledge of relationships between statistical measures, such as averages of variables, product of variables, correlations and joint probabilities. Examples of such averages are the mean velocity field, the mean wall stress, the heat flux, the local mean square velocity fluctuations, power spectra of velocities and so forth. Modern electronics and computers now enable us to determine many more statistical measures from experiments.

One has to be careful not to be misled by looking at averages, since averages may hide rather than reveal the physics of a process. An absurd example may serve as an illustration. Say that a blind man using a road bed sensor attempted to find out what motor vehicles looked like. Happening to use a road only traveled by airport limousines and motorcycles, he concludes that the average vehicle is a compact car with 2.4 wheels. He might later attempt to construct a theoretical model of the mechanics of such a vehicle, and may attain fame for a tentative model that looks like a motorcycle with a sidecar whose wheel is only in contact with the ground forty percent of the time.

In turbulent shear flow, this kind of a vehicle has been called an "average eddy," and may or may not exist. The desire to interpret a random process in terms of describable discrete events is easily understood; we must however always keep the physics in mind to avoid misleading ourselves.

In my attempt to explain the physics of events in turbulence, I shall start with the processes of instability and transition, where events occur in a more orderly fashion, and often in isolation, and then use the descriptions of the physics of such processes as elements for describing turbulent flows.

Next, some examples of how one can interfere with these processes by changes in boundary conditions and changes in fluid characteristics will be mentioned, as well as some comments on what are the important variables in a few of the engineering problems.

II. Process of Instability and Transition of a Laminar Boundary Layer

The ideal case of the instability of a laminar flow was investigated by Tollmien,[1] Schlichting,[2] Lin,[3] and others. They found that beyond a certain Reynolds number travelling waves of velocity fluctuations could develop and grow with downstream distance (Fig. 1).

Next, as analyzed by Benney and Lin,[4] and observed by Schubauer, Klebanoff,[5] and others, spanwise disturbances cause local free shear layers to form which cause bursts of high-frequency instability fluctuations, described by Klebanoff et al.[6] The very high growth rate of such local instability was analyzed, if not explained by Greenspan and Benney.[7] Next, the flow erupts locally into the Emmons'

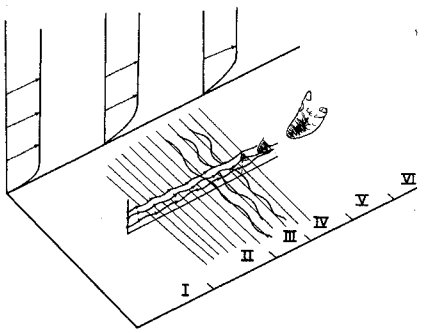

Fig. 1 Regions of instability and transition in laminar boundary layer: I) stable; II) Tollmien-Schlichting waves; III) Benney-Lin waves; IV) secondary breakdown; V) Emmons spots.

Presented as Paper 70-1308 at the AIAA 7th Annual Meeting and Technical Display, Houston, Texas, October 19–22, 1970; submitted December 29, 1970; revision received March 31, 1971. This lecture has drawn strongly on Kline's pioneering work on bursts in the turbulent boundary layer; the cooperation of the authors who have permitted me to show their results is also acknowledged. My own work on the subject has been supported by the National Science Foundation under Grant 4321 and by the Office of Naval Research (Contract Nonr-N00014-67-A-0204-0024). Last, but not least, I wish to thank the AIAA for providing me with this opportunity to make an attempt at surveying where we are in the problem of turbulent flow.

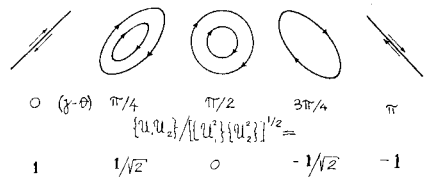

Fig. 2 Phase angles between $\mathfrak{U}_1$ and $\mathfrak{U}_2$ fluctuations and resulting Reynolds stress.

spots,[8] which further downstream causes such a confused flow that we call it turbulent.

In the stable regime, the flow can be described in terms of a steady velocity field, $\mathbf{U}(\mathbf{x})$. The instability, the Tollmien-Schlichting waves, superimposes a fluctuating velocity field $\mathfrak{U}(\mathbf{x},t)$; the Benney-Lin waves add yet two more velocity fields, one steady and one unsteady; next the bursts of local secondary instability add yet another, which distorts everything already there. How velocity fields interact by exchange of energy and vorticity is a basic element in the physics of instability and turbulence.

II.1 Decomposition of the velocity field

Consider a total velocity field $\mathbf{Q}(\mathbf{x},t)$ with Cartesian component Q_i and an associated pressure field Π. Let $\mathbf{Q}$ be composed of two velocity fields

$$\mathbf{Q}(\mathbf{x},t) = \mathbf{U}(\mathbf{x},t) + \mathfrak{U}(\mathbf{x},t) \tag{2.1}$$

and similarly for the pressure field

$$\Pi(\mathbf{x},t) = P(\mathbf{x},t) + \mathfrak{P}(\mathbf{x},t) \tag{2.2}$$

and assume that the scales over which the fields change are sufficiently different that they can be distinguished by taking spatial averages, say over a few wavelengths of $\mathbf{U}$ in the mean stream direction. Denoting this averaging process by braces, $\{\ \}$, it shall be characterized by

$$\{\mathfrak{U}_i\} = 0; \qquad \{\mathfrak{P}\} = 0$$

Thus,

$$U_i = \{Q_i\}\rangle \qquad P = \{\Pi\} \tag{2.3}$$

The equations of motion, taking the flow to be incompressible, are

$$\partial Q_i/\partial t + Q_j(\partial Q_i/\partial x_j) = -(1/\rho)(\partial\Pi/\partial x_i) + \nu\nabla^2 Q_i \tag{2.4}$$

$$\partial Q_i/\partial x_i = 0 \tag{2.5}$$

The equation for the vorticity $\boldsymbol{\zeta} = \text{curl}\ \mathbf{U}$ is

$$\frac{\partial\zeta_i}{\partial t} + Q_j\frac{\partial\zeta_i}{\partial x_j} = -\frac{1}{\rho}\frac{\partial\Pi}{\partial x_i} + \nu\nabla^2\zeta_i + \zeta_j\frac{\partial Q_i}{\partial x_j} \tag{2.6}$$

where the summation conventions have been used. Alternatively, the equations can be written in vector form:

$$\partial\mathbf{Q}/\partial t + (\mathbf{Q}\cdot\nabla)\mathbf{Q} = -(1/\rho)\nabla\Pi + \nu\nabla^2\mathbf{Q} \tag{2.4I}$$

$$\nabla\cdot\mathbf{Q} = 0 \tag{2.5I}$$

$$\partial\boldsymbol{\zeta}/\partial t + (\mathbf{Q}\cdot\nabla)\boldsymbol{\zeta} = (\boldsymbol{\zeta}\cdot\nabla)\mathbf{Q} + \nu\nabla^2\boldsymbol{\zeta} \tag{2.6I}$$

II.2 Reynolds Stress

Substituting for Q_i and Π into Eq. (2.4) and averaging one obtains Reynolds' equation

$$\frac{\partial U_i}{\partial t} + U_j\frac{\partial U_i}{\partial x_j} = -\frac{1}{\rho}\frac{\partial P}{\partial x_i} - \frac{\partial}{\partial x_j}\{\mathfrak{U}_i\mathfrak{U}_j\} + \nu\nabla^2 U_i \tag{2.7}$$

after taking account of the continuity equation (2.5) which yields

$$\partial\mathfrak{U}_i/\partial x_i = 0$$

This shows the effect of Reynolds stress $\{\mathfrak{U}_i\mathfrak{U}_j\}$ on the mean flow; the second term on the right of Eq. (2.7) gives the effect of momentum transport by fluctuations, which appears to the mean flow as an additional stress added to the pressure and the viscous stress terms. In the case of Tollmien-Schlichting waves, the fluctuations are almost periodic in the streamwise direction, x_1 and their angles and amplitudes are functions of the distance from the flat plate x_2; one may write:

$$\mathfrak{U}_1(x_1,x_2,t) = A(x_2)\cos[\alpha(x_1 - ct) + \gamma(x_2)]$$

$$\mathfrak{U}_2(x_1,x_2,t) = B(x_2)\cos[\alpha(x_1 - ct) + \vartheta(x_2)]$$

Evaluating the Reynolds stress, one obtains

$$\{\mathfrak{U}_1\mathfrak{U}_2\} = \tfrac{1}{2}A(x_2)B(x_2)\cos[\gamma(x_2) - \vartheta(x_2)] \tag{2.8}$$

Thus, there is no Reynolds stress when the oscillations are $\pi/2$ or $3\pi/2$ out of phase; the maximum stress occurs when the oscillations are in phase for given amplitudes of oscillation. Choosing a coordinate system which moves with the disturbances, so as to take out the oscillatory part of the disturbance field, the disturbance will appear as closed streamline fields. One can then draw pictures of fields with different relative phase of $\mathfrak{U}_1$ and $\mathfrak{U}_2$ (Fig. 2), and see how the inclination of an eddy disturbance affects the Reynolds stress, as pointed out by Starr.[9]

II.3 Energy Exchange

Next examine the energy relationships between the mean flow and the disturbances. In Eq. (2.4), substitute for Q_i and π, multiply by first U_i and average, then by $\mathfrak{U}_i$ and average, to obtain, after some manipulation:

$$\frac{\partial E}{\partial t} = -U_j\frac{\partial\{\mathfrak{U}_i\mathfrak{U}_j\}}{\partial x_j} - \nu\frac{\partial U_i}{\partial x_j}\frac{\partial U_i}{\partial x_j} + \frac{\partial}{\partial x_j}\left[-\frac{PU_j}{\rho} + U_jE + \frac{\nu}{2}\frac{\partial E}{\partial x_j}\right] \tag{2.9}$$

and

$$\frac{\partial\{\mathcal{E}\}}{\partial t} = -\{\mathfrak{U}_i\mathfrak{U}_j\}\frac{\partial U_i}{\partial x_j} - \nu\left\{\frac{\partial\mathfrak{U}_i}{\partial x_j}\frac{\partial\mathfrak{U}_i}{\partial x_j}\right\} + \frac{\partial}{\partial x_j}\left[\frac{-\{\mathfrak{P}\mathfrak{U}_j\}}{\rho} + U_j\{\mathcal{E}\} + \{\mathfrak{U}_j\mathcal{E}\} + \frac{\nu}{2}\frac{\partial\mathcal{E}}{\partial x_j}\right] \tag{2.10}$$

E is the kinetic energy density per unit mass in the mean flowfield, $E = U_iU_i/2$; $\mathcal{E}$ the kinetic energy density of the fluctuations, $\mathcal{E} = \mathfrak{U}_i\mathfrak{U}_i/2$; $D = \nu(\partial U_i/\partial x_j)\partial U_i/\partial x_j$ is the rate of viscous dissipation of energy per unit mass due to the mean motion; and $\mathfrak{D} = \nu(\partial\mathfrak{U}_i/\partial x_j)\partial\mathfrak{U}_i/\partial x_j$ is similarly the dissipation function for the fluctuations, namely the average product of viscous stress times strain.

Equations (2.9) and (2.10) show that the fluctuations, through the Reynolds stresses, change E and $\{\mathcal{E}\}$, that E and $\{\mathcal{E}\}$ also decay due to viscous dissipation. The third term on the right in each of the equations is a divergence term, thus integrating over a volume bounded by a surface S where the term in the square brackets is zero, one finds that the integral is zero, and the term makes no contribution to the total energy, but only distributes it among velocity components.

We shall do this for Eq. (2.10) where the integration volume is possible to specify. Thus, integrate instantaneously over the volume limited by the solid boundary, of extent one wavelength in the streamwise direction and a surface well into the freestream, to obtain

$$(\partial/\partial t)\iiint\mathcal{E}dV = -\iiint\mathfrak{U}_i\mathfrak{U}_j(\partial U_i/\partial x_j)dV - \iiint\mathfrak{D}dV + \iint_D[-\mathfrak{P}\mathfrak{U}_j/\rho + U_j\mathcal{E} + \mathfrak{U}_j\mathcal{E} - \nu\,\partial\mathcal{E}/\partial x_j]n_jdS$$

The surface integral is zero, since the integrand vanishes on the boundary and in the freestream, as well as on nodal lines of the $\mathfrak{U}$-field, where we placed the vertical boundaries. We

are thus left with

$$(\partial/\partial t) \iiint \mathcal{E} dV = -\iiint (\mathfrak{U}_i \mathfrak{U}_j (\partial U_i/\partial x_j) + \mathfrak{D}) dV \quad (2.11)$$

Introducing a velocity scale U_0 and a length scale δ, this becomes, in nondimensional form:

$$(\partial/\partial t') \iiint \mathcal{E}' dV = -\iiint \mathfrak{U}_i' \mathfrak{U}_j' (\partial U_i'/\partial x_j') dV - (1/Re) \iiint \mathfrak{D}' dV \quad (2.12)$$

where $Re = U_0\delta/\nu$, the Reynolds number, and the primes denote nondimensional variables.

The growth of an instability is thus governed by a balance between production and dissipation, this balance being directly dependent upon Reynolds numbers, but the production term is also dependent upon the relative phase of velocity oscillations, which is affected by viscosity. There is for each laminar flow a critical Reynolds number where it goes unstable. Squire[10] has shown that for infinitesimal disturbances, it is the two-dimensional disturbance that is the most unstable, since the Reynolds number which appears in Eq. (2.12) for oblique disturbance with wave propagation direction ϑ to the mean stream is $Re \cos\vartheta$, thus the flow is most unstable for $\cos\vartheta = 0$. For finite disturbances, which affect the mean flow, this is not the case. This is the reason we have retained Eq. (2.12) in a form valid for three-dimensional disturbances.

II.4 Vorticity Exchange

Equation (2.6[1]) shows that the total rate of change of vorticity on the left is equal to the effect of stretching and tilting of vortex lines (the first term on the right) plus viscous diffusion. Tilting a vortex line changes its direction, and therefore the relative magnitude of vorticity components; stretching a vortex line concentrates the vorticity in a smaller volume. Both effects are of crucial importance in the development of boundary-layer transition.

To show that the fluctuations also change the mean vorticity, set $Q_i = U_i + \mathfrak{U}_i$ in Eq. (2.6), multiply by Ω_i, where $\Omega = \text{curl } \mathbf{Q}$ and average to obtain

$$\left(\frac{\partial}{\partial t} + U_j \frac{\partial}{\partial x_j}\right) \frac{\Omega_i \Omega_i}{2} - \Omega_i \Omega_j \frac{\partial U_j}{\partial x_i} + \Omega_i \epsilon_{ijk} \frac{\partial^2}{\partial x_j \partial x_\alpha} \{\mathfrak{U}_\alpha \mathfrak{U}_k\} = \nu \Omega_i \nabla^2 \Omega_i \quad (2.13)$$

where ϵ_{ijk} is the alternating tensor. The first term is the vorticity transport term, the second contains stretching and tilting, and the third gives the effect of Reynolds stress torque working on mean rotation and the right hand term effects of diffusion. Thus, the Reynolds stresses due to fluctuations will change the mean vorticity level.

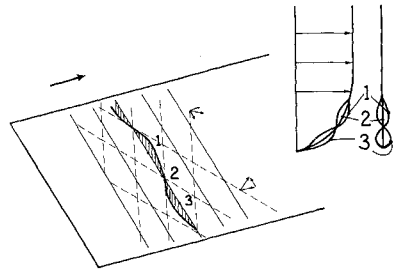

Fig. 3 Oblique waves forming spanwise standing, streamwise travelling waves.

III. Three-Dimensional Disturbances

The Tollmien-Schlichting waves grow exponentially with distance or with time as measured if one rides on a wave. This can be seen from Eq. (2.11), since for infinitesimal disturbances, where a linear approximation is valid, $\{\mathfrak{U}_i \mathfrak{U}_j\}$ will be proportional to $\{\mathcal{E}\}$ and $\partial U_i/\partial x_j$, will be unaffected by the oscillations. $\mathfrak{D}$ will also be proportional to $\{\mathcal{E}\}$, so one finds

$$\partial\{\mathcal{E}\}/\partial t \sim \beta\{\mathcal{E}\}$$

and therefore

$$\{\mathcal{E}(t)\} = \{\mathcal{E}\} \exp[\beta t] \quad (3.1)$$

The disturbance will therefore grow this way until the mean flow is affected.

We can look at this effect the following way: Say that Squire's theorem breaks down, so that the most unstable oscillations are oblique waves. Since nature does not know the difference between right and left, one must expect two families of oblique waves to occur, as indicated in Fig. 3. This wave field adds up to standing waves spanwise travelling in the streamwise direction. In addition, the two-dimensional Tollmien-Schlichting waves that arose further upstream will also be present.

Let us ignore them for the moment, and say that the mean flow is $\mathbf{U}$ and the oblique waves are $\mathfrak{U}$. $\mathfrak{U}$ is periodic spanwise, thus the Reynolds stress term in Eq. (2.7) is periodic spanwise,

$$\frac{\partial U_i}{\partial t} + U_j \frac{\partial U_i}{\partial x_j} = -\frac{1}{\rho}\frac{\partial P}{\partial x_i} - \frac{\partial}{\partial x_j}\{\mathfrak{U}_i \mathfrak{U}_j\} + \nu \nabla^2 U_i \quad (2.7)$$

thus inducing a spanwise variation in the $\mathbf{U}$-field. Equation (2.10) shows that a spanwise variation of U_1, in the form $\partial U_i/\partial x_3$ will give a production term:

$$\{\mathfrak{U}_i \mathfrak{U}_3\} \partial U_i/\partial x_3$$

thus affecting the growth rate and in turn the Reynolds stresses which will change the mean velocity field.

This type of nonlinear instability, where the disturbance changes the mean flow so as to enable it to increase its growth,

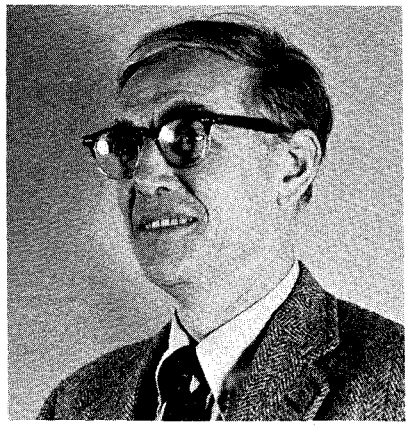

Erik Mollo-Christensen

Erik Mollo-Christensen was born in Norway, educated at Oslo University and at M.I.T. (S.B. 1948, S.M. 1949 in Aeronautical Engineering, Sc.D. in 1954). He worked from 1949 to 1951 at the Norwegian Defense Research Establishment, was a Senior Scientific Officer when he left in 1951 to return to M.I.T. He was appointed to the faculty at M.I.T. in 1955, spent a year at Caltech as Senior Research fellow while on a J. S. Guggenheim Foundation Fellowship. He became Professor of Aeronautics at M.I.T. in 1962 and transferred to the Department of Meteorology in 1964.

He has worked on aeroelasticity, unsteady aerodynamics, turbulence, sound generation, the atmospheric boundary-layer and air-sea interaction, principally as an experimenter. He is a member of AIAA, AMS, AGU, AIP and the American Academy of Arts and Sciences.

He served as a member and later as Chairman (1968) of the National Committee for Fluid Mechanics Films. His film "Flow Instabilities" was awarded the "Golden Eagle" by the Council on International Non-Theatrical Events in 1969 and has won several awards at film festivals abroad.

He is the 1970 recipient of the Von Kármán Award from the AIAA.

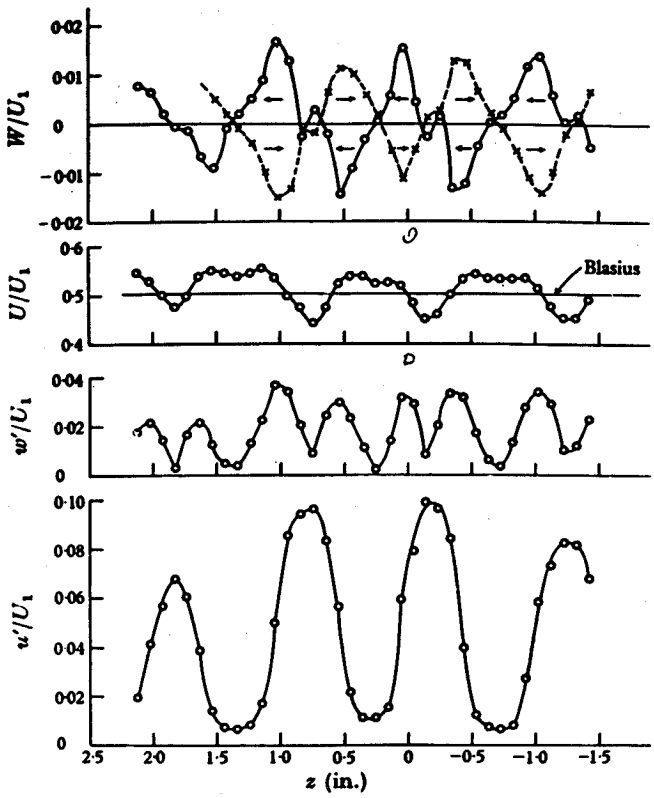

Fig. 4 Spanwise distribution of mean and fluctuating velocity components. z is spanwise distance. —— y = 0.31, - - - y = 0.11 (from Ref. 6). w' and W are spanwise velocities.

was analyzed by Benney[4] and observed by Schubauer and Klebanoff.[5] The presence of the Tollmien-Schlichting waves plays a crucial role in this phenomenon, but we shall postpone explanations and first look at some data.

Figure 4 shows mean and fluctuating components of velocity as functions of spanwise distance, as obtained by Klebanoff, Tidstrom and Sargent.[6]

The average vorticity equation

$$\left(\frac{\partial}{\partial t} + U_j \frac{\partial}{\partial x_j}\right)\Omega_i - \Omega_j \frac{\partial U_i}{\partial x_j} - \nu\nabla^2\Omega_i = - \epsilon_{ijk} \frac{\partial^2\{u_\alpha u_k\}}{\partial x_j \partial x_\alpha} \quad (3.2)$$

shows that there will be a vorticity periodicity spanwise in the presence of a periodicity of Reynolds stress. But if the mean flow varies spanwise, the vorticity must be advected at different speeds at different spanwise positions, thus vortex lines, in order to remain continuous, must be stretched, thus increasing locally some of the terms $\partial U_i/\partial x_j$ as well as U_i due to vortex stretching. Equation (2.10) shows that this will change both $\{u_i u_j\}$ and $\partial U_i/\partial x_j$ in the production term, and thus the growth rate of disturbances $\partial\{\mathcal{E}\}/\partial t$.

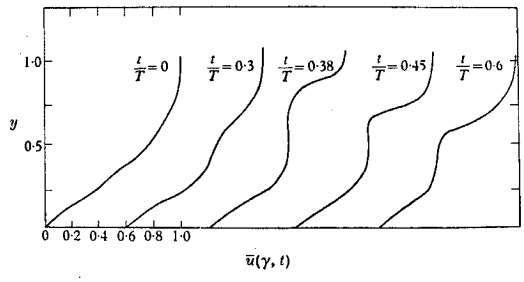

Fig. 5 Instantaneous velocity profiles at onset of secondary instability (from Ref. 11).

To recapitulate, a three-dimensional disturbance of finite amplitude may modify the mean flow so as to enhance its own growth rate and the rate of modification of the mean flow. This process sets the stage for intermittent appearance of local instabilities, which is the next stage in boundary layer development.

IV. Local Bursts of Instability

The combined effects of the spanwise periodic distortion of the mean flow and the spanwise varying amplitude and form of the fluctuations travelling downstream finally grow to a magnitude which causes the instantaneous velocity profiles in certain spanwise locations to have local inflection points, as shown in Fig. 5, from Kovasznay.[11] Linear analysis shows that a free shear layer, that is a flow with an inflection point in the velocity profile, is unstable.

If one tries to determine the growth rate of these secondary instabilities for a steady, parallel flow with a profile corresponding to the instantaneous profile observed, one finds a growth rate orders of magnitude smaller than that observed. Greenspan and Benney[7] have analyzed the instability of a free shear layer of oscillating thickness by numerical means. They found that indeed the energy of the secondary instabilities grows much faster than instabilities in a steady flow, as shown in Fig. 8, where the ratio of the fluctuation energy to that for a corresponding steady flow is plotted for part of a period of the basic oscillation.

This deserves a further explanation, since it most likely describes a phenomenon which also occurs in turbulent flow. In order to examine the energy and vorticity relationships, we shall have to consider the interactions of three velocity fields, a steady one, a long wave fluctuation and a very short wave fluctuation.

IV.1 Decomposition of Velocity Field into Three Fields

Let the total velocity field be described in terms of three fields:

$$\mathbf{Q}(\mathbf{x},t) = \mathbf{U}(\mathbf{x},t) + \mathbf{U}(\mathbf{x},t) + \mathbf{u}(\mathbf{x},t) \quad (4.1)$$

with the corresponding pressure fields:

$$\Pi(\mathbf{x},t) = P(\mathbf{x},t) + \mathcal{P}(\mathbf{x},t) + p(\mathbf{x},t) \quad (4.2)$$

and let the scales of the three component fields be respectively L, $\mathcal{L}$ and l, where

$$L \gg \mathcal{L} \gg l \quad (4.3)$$

and the time scales of fluctuation be similarly dissimilar (Fig. 7). Assume that the velocity fields can be distinguished by averaging over different length or time scales.

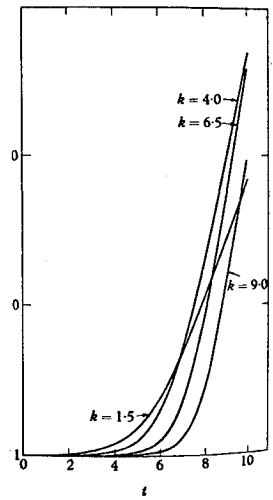

Fig. 6 Growth of energy of fluctuations in time dependent shear layer divided by growth rate in steady shear layer (from Ref. 4).

An average over many length or time scales of $\mathbf{u}$, but over a fraction of the scale of $\mathbf{U}$ will be denoted by angular brackets, $\langle\ \rangle$. This is arranged so as to yield

$$\langle u_i \rangle = 0; \qquad \langle \mathfrak{U}_i \rangle = \mathfrak{U}_i; \qquad \langle U_i \rangle = U_i \tag{4.4}$$

Thus, the small scale averages of the larger scale fields are indistinguishable from the fields themselves. This is, of course, an approximation to any real flow.

Next, define an average over many periods of $\mathfrak{U}$, but over much less than the time constant of change of the mean flow, by braces $\{\ \}$. This averaging procedure has the characteristics:

$$\{U_i\} = U_i; \qquad \{\mathfrak{U}_i\} = 0; \qquad \{u_i\} = 0 \tag{4.5}$$

Further properties of the averages are

$$\begin{gathered} \{\mathfrak{U}_i\mathfrak{U}_j\} \neq 0; \qquad \langle u_i u_j \rangle \neq 0 \\ \{\langle u_i u_j \rangle\} \neq 0; \ \{\mathfrak{U}_i u_j\} = 0 \end{gathered} \tag{4.6}$$

This allows us to consider the mean effect of small scales on larger scales and vice versa.

From the momentum Eq. (2.4), one obtains, after substitution, multiplying by U_i, $\mathfrak{U}_i$ and u_i respectively, averaging and some further manipulation, the three energy equations:

$$\frac{\partial E}{\partial t} = -U_i \frac{\partial}{\partial x_j} (\{\mathfrak{U}_i\mathfrak{U}_j\} + \{\langle u_i u_j \rangle\}) - D + \frac{\partial}{\partial x_j}\left[-\frac{PU_j}{\rho} + U_j E + \frac{\nu}{2}\frac{\partial E}{\partial x_j}\right] \tag{4.7}$$

$$\frac{\partial \{\mathcal{E}\}}{\partial t} = -\left(\{\mathfrak{U}_i\mathfrak{U}_j\}\frac{\partial U_i}{\partial x_j} - \left\{\mathfrak{U}_i \frac{\partial \langle u_i u_j \rangle}{\partial x_j}\right\}\right) - \{\mathfrak{D}\} + \frac{\partial}{\partial x_j}\left[-\frac{\{\mathfrak{P}\mathfrak{U}_j\}}{\rho} + U_j\{\mathcal{E}\} + \{\mathfrak{U}_j\mathcal{E}\} + \frac{\nu}{2}\frac{\partial\{\mathcal{E}\}}{\partial x_j}\right] \tag{4.8}$$

$$\frac{\partial \langle e \rangle}{\partial t} = -\langle u_i u_j \rangle\left(\frac{\partial U_i}{\partial x_j} + \frac{\partial \mathfrak{U}_i}{\partial x_j}\right) - d + \frac{\partial}{\partial x_j}\left[-\frac{\langle p u_j \rangle}{\rho} + (U_j + \mathfrak{U}_j)\langle e \rangle + \langle u_j e \rangle + \frac{\nu}{2}\frac{\partial \langle e \rangle}{\partial x_j}\right] \tag{4.9}$$

where

$$E = U_i U_i/2; \qquad \mathcal{E} = \mathfrak{U}_i\mathfrak{U}_i/2; \qquad e = u_i u_i/2$$

and

$$D = \nu \frac{\partial U_i}{\partial x_j}\frac{\partial U_i}{\partial x_j}; \qquad \mathfrak{D} = \nu \frac{\partial \mathfrak{U}_i}{\partial x_j}\frac{\partial \mathfrak{U}_i}{\partial x_j}$$

$$d = \nu \frac{\partial u_i}{\partial x_j}\frac{\partial u_i}{\partial x_j}$$

are the corresponding dissipation functions.

Equations (4.7), (4.8) and (4.9) equate the rate of change of kinetic energy per unit mass in each mode of motion to: An interaction term, the first term on the right, a dissipation term D, $\mathfrak{D}$, d, respectively, and a divergence term in square brackets.

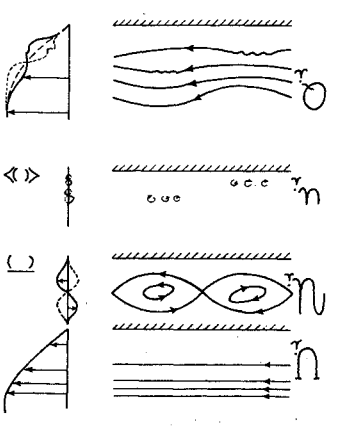

Fig. 7 Decomposition of velocity field into three fields.

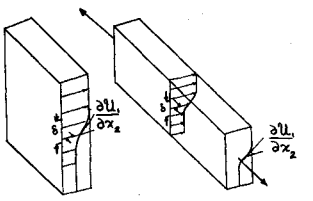

Fig. 8 Increase in vorticity by vortex stretching.

The divergence term contains the work done by pressure gradients, one or more advection of energy terms and finally an energy diffusion term, which for Eq. (4.8), for example, is

$$\nu \frac{\partial^2}{\partial x_j \partial x_j}\{\mathcal{E}\} = \nu\nabla^2\mathcal{E}$$

The averaging is equivalent to an integration over suitable volumes. If the instabilities occur in isolated patches, it is possible to define the averaging volume such that the disturbances vanish on the bounding surface, and the divergence terms have a zero contribution to the average energy balance. However, they do play an important role in redistributing energy between velocity components and scales. We shall ignore the divergence terms, which in effect amounts to saying that we limit the discussion to times when the bursts of turbulence are isolated.

The production terms containing the interaction between pairs of modes add up to divergence terms, thus showing that energy is indeed exchanged. For example, adding the terms with $\mathbf{U}$ in Eqs. (4.7) and (4.8) gives:

$$-U_i \frac{\partial}{\partial x_j}\mathfrak{U}_i\mathfrak{U}_j - \mathfrak{U}_i\mathfrak{U}_j\frac{\partial U_i}{\partial x_j} = -\frac{\partial}{\partial x_j}(\mathfrak{U}_i\mathfrak{U}_j U_i)$$

a divergence which will vanish upon integration over a suitably defined volume.

IV.2 Effect of Primary Oscillation on Secondary Instability Growth

First, let us observe that in order to thin down a shear layer at one spanwise position without changing the mean velocity difference across it, it must be stretched in the spanwise direction (Fig. 8). This increases the vorticity, both in the mean flow, which is three-dimensional in the primary fluctuations $\mathfrak{U}$, as well as the secondary instability vorticity curl $\mathbf{u}$. Thus, thinning a shear layer by stretching it laterally will increase the amplitude of the secondary instability proportional to the amount of lengthening of the stream tubes. This is only part of the amount of lengthening of the stream tubes. This is only part of the effect, as can be seen from Eq. (4.9). Ignoring the divergence term, for the reasons stated earlier, we see that the growth rate of $\langle e \rangle$ is proportional to $\partial\mathfrak{U}_i/\partial x_j$, which contains terms describing the primary vorticity fluctuations. Thus $\partial\langle e \rangle/\partial t$ is changed by changes in $\partial\mathfrak{U}_i/\partial x_j$.

Further, looking at the production term in Eq. (4.8):

$$-\{\mathfrak{U}_i \partial\langle u_i u_j \rangle/\partial x_j\}$$

we see that if a secondary instability occurs periodically on a primary instability, the primary instability can grow due to the work done by the Reynolds stresses of the secondary fluctuations. We can illustrate the interaction by a block diagram (Fig. 9), which schematically shows how $\{\mathcal{E}\}$ governs $\mathfrak{U}_i$, which pushing against the Reynolds stress $\langle u_i u_j \rangle$, governed by and crudely, for selfsimilar growth, proportional to $\langle e \rangle$, puts energy into $\{\mathcal{E}\}$, while the interaction $\langle u_i u_j \rangle \partial\mathfrak{U}_i/\partial x_j$ feeds $\langle e \rangle$.

This interaction may therefore enhance the growth of both u and $\mathfrak{U}$, also enabling both to extract energy more efficiently from the large scale velocity field. This is achieved through

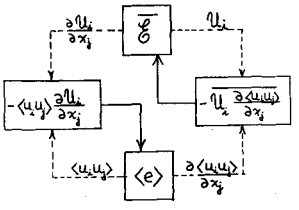

Fig. 9 Block diagram of interactions between fluctuations of different scales.

the terms

$$-\{\mathfrak{U}_i\mathfrak{U}_j\}\partial U_i/\partial x_j \qquad \text{in Eq. (4.8)}$$

and

$$-\langle u_i u_j\rangle \partial U_i/\partial x_j \qquad \text{in Eq. (4.9)}$$

This removal of energy cannot go on forever, since the large scale flow will react. Its energy density will change due to the production terms in Eq. (4.7); the flow will be accelerated, as can be seen from Reynolds' equation:

$$\frac{\partial U_i}{\partial t} + U_j\frac{\partial U_i}{\partial x_j} + \frac{1}{\rho}\frac{\partial P}{\partial x_i} - \nu\nabla^2 U_i = -\frac{\partial}{\partial x_j}\left[\{\langle u_i u_j\rangle\} + \{\mathfrak{U}_i\mathfrak{U}_j\}\right] \quad (4.10)$$

This equation, together with Eqs. (4.7), (4.8) and (4.9) illustrate a crucial fact about instability and turbulence which is not mentioned much in the literature, namely that:

Reynolds stress is associated with generation of fluctuations. No generation—no stress, no stress—no generation. This says that in order to understand Reynolds stress, we have to understand generation of fluctuations.

The generation of fluctuations also changes the vorticity in the large scale flow. We see this by introducing the different vorticity fields into the vorticity equation, taking the scalar product of the large scale vorticity and averaging.

Decompose the total vorticity

$$\text{curl } \mathbf{Q} = \boldsymbol{\zeta} = \mathbf{W} + \mathfrak{W} + \mathbf{w}$$

to obtain, from Eq. (2.6), after averaging and manipulating:

$$\left(\frac{\partial}{\partial t} + U_j\frac{\partial}{\partial x_j}\right)\frac{W_i W_i}{2} - W_i W_j\frac{\partial U_i}{\partial x_j} - \nu W_i\nabla^2 W_i = -W_i\epsilon_{ijk}\frac{\partial^2}{\partial x_j\partial x_\alpha}\left[\{\mathfrak{U}_\alpha\mathfrak{U}_k\} + \{\langle u_\alpha u_k\rangle\}\right] \quad (4.11)$$

The first term is the substantial rate of change of mean square vorticity, the second term is the vortex stretching and tilting term, the third term is due to vortex diffusion. The term on the right describes the torque from the Reynolds stresses working against the large scale rotation of fluid elements.

It is therefore reasonable to expect that the combined effects of primary and secondary instability will change the large scale flowfield quickly and radically, exhausting the available vorticity for further growth, and causing a new distortion of the velocity field, the Emmons' spot.[8]

The regions of intense production occur periodically spanwise and travel in the downstream direction. High production regions are high Reynolds stress regions. They move first at the speed of the Tollmien-Schlichting waves, that is more slowly than the mean stream above, and faster than the mean flow closer to the boundary. The production regions therefore look like obstacles to the flow above and below.

A shear flow encountering an obstacle forms a horseshoe vortex around it. A moving obstacle should form two sets of horseshoe vortices which may partially join. Since this process is so poorly understood, I shall not attempt to describe it; observations show that the flow erupts violently in a three-dimensional manner.

Figure 10 shows a hydrogen bubble picture of a similar event obtained by Kim, Kline and Reynolds.[12]

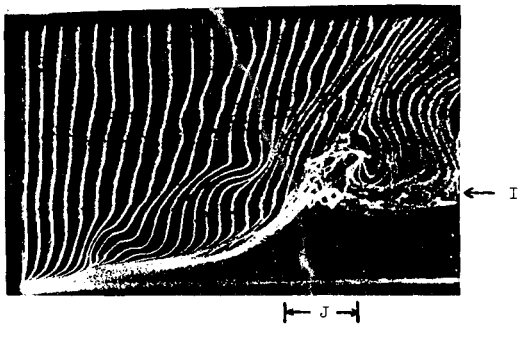

Fig. 10 Breakup following a burst of instability (from Ref. 11).

IV.3 Recapitulation

We have made plausible even if not proved, that the occurrence of secondary instability can enhance the growth rate of a primary instability and vice versa, that the combined effect upon the large scale flow may exhaust the available vorticity and modify the large scale velocity field strongly. It has also been shown that Reynolds stress and turbulence production are inseparable events.

V. Turbulent Flows

We know many of the technically important facts about turbulent boundary layers and some other turbulent flows. For example, the drag caused by a turbulent boundary layer can be closely estimated, the heat transfer from a tube wall to a turbulent pipeflow is sufficiently well-known to design heat exchanges and we have learned to handle other problems of design of equipment involving flow by a mixture of empirically obtained similarity laws and crude theory.

The question of why we should want to know more than the mean or average effects in turbulent flow naturally arises. First, because even in technical applications, the time-dependent random events are important. For example, structural vibration induced by turbulent fluctuations involve both the time-dependent stresses on structures and the response of turbulent flows to time-dependent boundary conditions. The erosion of a sand bed is not caused by the average stress; the particles are dislodged by the intermittently occurring large stresses. In aerodynamic noise, it is the fluctuating stresses on fluid particles that react on the surrounding medium to emit sound.

Second, if we shall ever understand how one can change the structure of a turbulent flow to, for example, lower drag, we must understand the dynamics of turbulence in order to be able to analyze and predict how flows are affected by compliant boundaries, long chain polymer additives, impinging sound and even unusual boundary geometry.

Finally, we want to understand more because of scientific curiosity, since turbulent flow is such an interesting example of strong interaction between scales of motion, and if we can reach a further partial understanding of such phenomena, we may get new methods in statistical mechanics, which can be

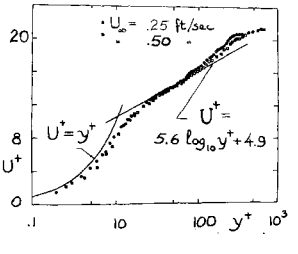

Fig. 11 Mean velocity profile in turbulent boundary layer. $U^+ = U(y)/u^+$; $y^+ = yu^+/\nu = x_2{}^+$ (from Ref. 12).

applied to a host of other phenomena, from social dynamics to plasma physics, to mention two extremes.

We shall therefore summarily describe some of the mean properties of the turbulent boundary layer to set the context for further description and speculation about the dynamics of turbulent flow.

V.1 A Cursory Description of the Mean Turbulent Boundary Layer

After transition occurs, the flow stays turbulent, the turbulence being maintained by intermittent local generation and by the more continuous generation by deformation of the turbulence by the mean flow. Most of the velocity fluctuations one observes at a given point in the flow was generated somewhere upstream and blown at the observer. If one tries to interpret the dynamics of generation by observing mostly the debris from generating events, and not the events themselves, one may be in danger of constructing the counterpart of the 2.4 wheeled motorcycle. Be this as it may, an average is an average, and the average properties of the turbulent boundary layer are well-known, due largely to the work of Theodore Von Kármán and improved upon by later workers.

The mean velocity profile over a smooth flat plate was found to be by Coles[13]:

$$\frac{U_1(x_2)}{u^+} = \frac{1}{K}\ln(1 + Kx_2) + \gamma\left[1 - e^{-x_2^+/\delta_v} - \frac{(x_2^+ e^{-0.33x_2^+})}{\delta_v}\right] + 1.38\left\{1 + \sin\left[\frac{\pi(2cx_2^+ - 1)}{2}\right]\right\}$$

where K is Von Kármán's constant, γ,δ_v are other nondimensional constants, and the length ν/u^+ has been used to make the distance from the surface dimensionless:

$$x_2^+ = x_2\nu/u^+$$

u^+ is the friction velocity, related to the wall shear stress τ_w by

$$\tau_w = \rho u^{+2}$$

Similarly, the wall friction coefficient c_f:

$$c_f = 2u^{+2}/U_\infty^2$$

varies with Reynolds number $R_x = U_\infty x_1/\nu$ approximately as

$$c_f = 0.370(\log_{10}R_x)^{-2.584}$$

which is a further development of a relation first obtained by Von Kármán.

Experimental data[12,14,15] on the shape of the mean velocity profile are shown in Fig. 11. The figure shows two of the distinct domains of the boundary layer; the sublayer near the wall, extending to approximately $x_2^+ = 30$, and a layer further out with a logarithmic velocity profile.

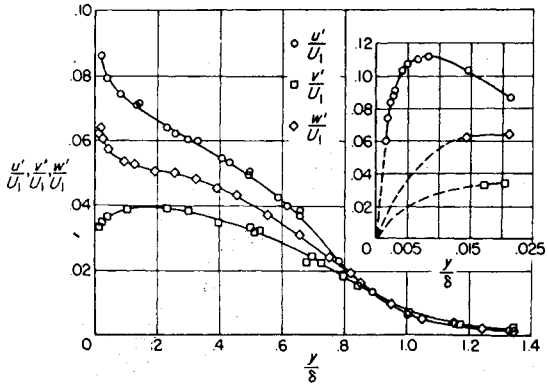

Fig. 12 Distribution of rms intensities of velocity components in turbulent boundary layers (from Ref. 14).

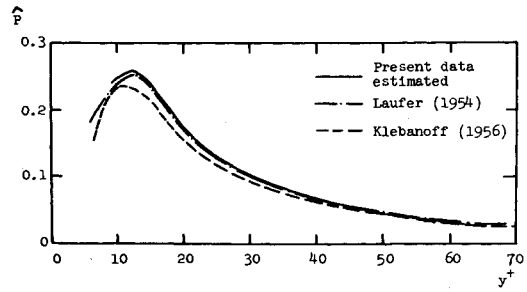

Fig. 13 Mean production of turbulence $\hat{P}$ vs distance from wall (from Ref. 12).

The Reynolds number of the sublayer, based on $x_2^+ = 30$, and the velocity there is approximately 900, thus marginally unstable, based on linear stability considerations. The drag coefficient changes very slowly with Reynolds number, the dominant dependence being logarithmic.

V.2 Fluctuations and Stresses

A typical distribution of root mean square intensity of fluctuations of velocity components are shown in Fig. 12. The intensity of u_1 is seen to be a maximum near the edge of the sublayer.

The distribution of production of turbulence[12,14,15] defined as

$$\hat{P} = -u_1u_2(\partial U_1/\partial x_2)\nu/u^{+4}$$

and plotted vs $y^+ = x_2^+$, it shown in Fig. 13. The production is a maximum near the outer edge of the sublayer.

The production of turbulence is an intermittent process, as has been shown by Kline, for example (Fig. 14), where production $\hat{P}(t)$ has been plotted vs time for different distances from the wall. Other data from a very interesting set of experiments by Kline[12] and his colleagues show that even at the low Reynolds number of their experiments ($R_x = 3.5 \times 10^5$ and 6.2×10^5) the production of turbulence seemed to be associated with bursts or eruptions reminiscent of Emmons' spots, that the production seemed to be dominated by the production in bursts (Fig. 15), and that bursts occurred separated in time (Fig. 16).

It is well-known that at very high Reynolds numbers, turbulence occurs intermittently; the data of Grant, Stewart and Moilliet[16] show this for oceanic turbulence. Some of our own data for the atmospheric boundary layer may serve as further illustration. Figure 17 shows some traces of turbulent velocity fluctuation above the sea surface for different fre-

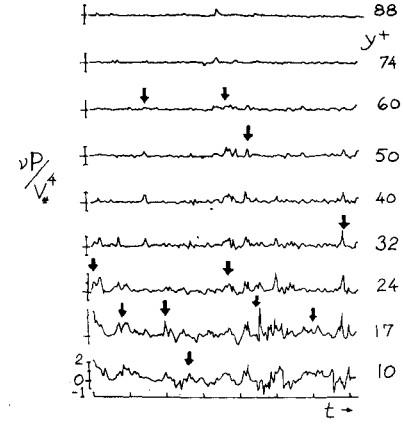

Fig. 14 Production $\hat{P}$ vs time at nine different heights in boundary layer, from top $y^+ = 88, 74, 60, 50, 40, 32, 24, 17,$ and 10 (from Ref. 12).

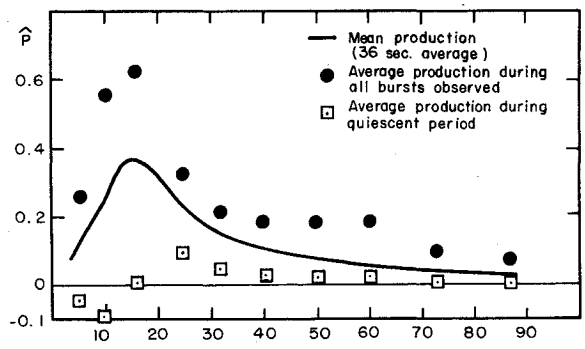

Fig. 15 Production $\hat{P}$ in bursts and between bursts vs. distance from the wall y^+ (from Ref. 12).

quency bands. If turbulence occurs intermittently at high Reynolds numbers (in this case $R_x = 10^{11}$), one must conclude that turbulent production is highly intermittent, and that the intermittency increases with Reynolds number.

In the following I shall discuss some of the mechanics of such events drawing on the evidence which is developing, but with the caution that I may be wrong in my interpretation.

VI. Suggested Mechanics of Bursts of Turbulent Production

The evidence obtained so far by many workers shows that generation of turbulence takes place in intermittent bursts, that bursts are associated with distortion of the velocity profiles, that bursts contain velocity fluctuations of a range of scales and that the intermittency, that is the time fraction of no production, increases with Reynolds number.

This suggests that bursts of turbulence production are in many ways similar to the events which precede and constitute transition to turbulent flow, namely that a local instability develops, which becomes three-dimensional, develops secondary instability and then changes the large scale flow radically.

VI.1 Reynolds Number

First, let us remind ourselves what Reynolds number is. Based on boundary-layer thickness, for example:

$$R_\delta = U_\infty \delta/\nu$$

or written differently:

$$\delta/(\nu/U_\infty) = \delta/l_v$$

δ is the boundary-layer thickness, l_v is another length, the length scale over which a velocity difference U_∞ is dominated by viscous effects. Stated differently, it is the length scale which makes the Reynolds number of a flow typified by a velocity U_∞ equal to unity.

Thus, the Reynolds number is a measure of the largest scale to the viscous dominated scale in a flow with a given typical velocity. At the critical Reynolds number for instability, the largest scale and the smallest undamped scale of fluctuation coincide.

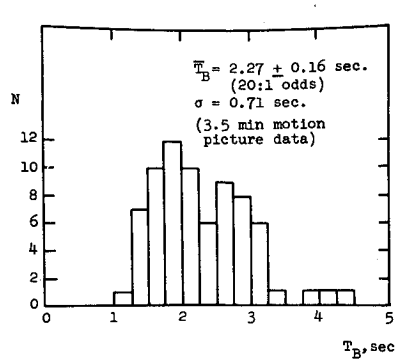

Fig. 16 Number N of occurrence of time T_B between bursts (from Ref. 12).

At higher Reynolds numbers, the ratio of large to viscous limit scales increases, partly due to changes of velocity profiles which then permit secondary instabilities. But where secondary instabilities do occur, it is of course possible that tertiary instabilities also can occur, and even higher orders, of still smaller scales.

One may guess that the number of participants in the hierarchy of instabilities that can occur increases with Reynolds number, but not very fast. A reasonable guess would be that in a free shear layer, the number of simultaneously participating instabilities should vary as the logarithm of the Reynolds number. Let λ_j be the wavelength of the jth instability; if we assume similarity in the instabilities:

$$\lambda_1/\lambda_2 = \lambda_2/\lambda_3 = \lambda_3/\lambda_4 = \ldots = \lambda_{N-1}/\lambda_N = \alpha^{-1}$$

we find

$$\lambda_N/\lambda_1 = \alpha^N$$

and

$$N \sim \log \lambda_N/\lambda_1$$

Taking λ_N/λ_1 to be a measure of the Reynolds number gives

$$N \sim \log Re_x \tag{6.1}$$

Thus, we may guess that it takes large changes in Reynolds numbers to make significant changes in the process of secondary instabilities which occur in a burst, and that therefore it is reasonable that the properties of a turbulent boundary layer vary so slowly with Re_x, and do in fact depend upon log Re_x.

Since the duration of a production burst and the interval between bursts depend upon Reynolds number, intermittency must be due to the efficiency of production and therefore the rate of exhaustion of available vorticity being dependent upon Reynolds number.

We shall therefore again look at what energy may reveal about interactions between scales of instability.

VI.2 Interactions in a Burst

Look again at Eqs. (4.7), (4.8) and (4.9), which we repeat here for convenience:

$$\frac{\partial E}{\partial t} = -U_i \frac{\partial}{\partial x_j}(\{\mathfrak{U}_i\mathfrak{U}_j\} + \{\langle u_i u_j\rangle\}) - D + \frac{\partial}{\partial x_j}[\mathfrak{U}]_j \tag{4.7}$$

$$\frac{\partial\{\mathcal{E}\}}{\partial t} = -\{\mathfrak{U}_i\mathfrak{U}_j\}\frac{\partial U_i}{\partial x_j} - \left\{\mathfrak{U}_j \frac{\partial\langle u_i u_j\rangle}{\partial x_j}\right\} - \{\mathfrak{D}\} + \frac{\partial}{\partial x_j}[\mathfrak{U}]_j \tag{4.8}$$

$$\frac{\partial\langle e\rangle}{\partial t} = -\langle u_i u_j\rangle\left(\frac{\partial U_i}{\partial x_j} + \frac{\partial \mathfrak{U}_i}{\partial x_j}\right) - \langle d\rangle + \frac{\partial}{\partial x_j}[u]_j \tag{4.9}$$

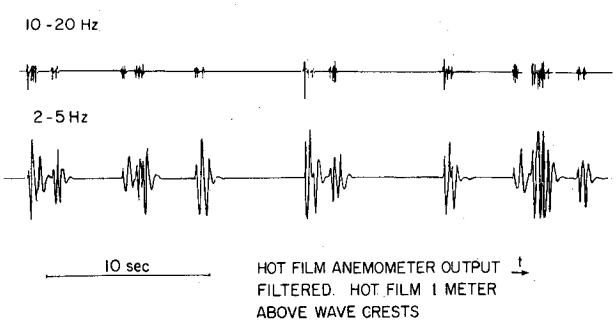

Fig. 17 Traces of velocity fluctuations in air boundary layer above sea surface as filtered through two nonoverlapping rectangular spectral windows.

We shall assume that at least for a certain portion of the lifetime of a burst of turbulence production it is possible to define three velocity fields of different scales, and we take these velocity fields to represent: U_i, the average large scale velocity field during the time interval we consider; $\mathfrak{U}_i$ the primary instability which occurs during the burst; and u_i, the secondary instability taking place at certain phases of the primary instability.

Again we shall neglect the effect of the divergence terms. We can then discuss the interactions during the first occurrence and early life of a burst.

The local large scale velocity profile may look like any one of three profiles on the right of Fig. 18, which shows profiles during a burst.

The primary instability may be Tollmien-Schlichting waves associated with the first occurring unstable profile, the one to the right, and the secondary instability connected with local instabilities of even shorter time average profiles.

As in laminar instability and transition, Eqs. (4.7)–(4.9) show that a primary instability may draw energy from the mean stream:

$$-\{\mathfrak{U}_i\mathfrak{U}_j\}\,\partial U_i/\partial x_j \qquad \text{(Eq.[4.7])}$$

that a secondary instability may increase the growth of the primary instability:

$$-\{\mathfrak{U}_i\,\partial\langle u_iu_j\rangle/\partial x_j\} \qquad \text{(Eq.[4.7])}$$

The straight growth of a primary instability, or three-dimensional growth which enhances the term $\partial\mathfrak{U}_i/\partial x_j$ even more, through vortex stretching, will help the growth of secondary instability through the term

$$-\langle u_iu_j\rangle\,\partial\mathfrak{U}_i/\partial x_j \qquad \text{(Eq.[4.9])}$$

The presence of secondary instability will therefore change the growth rate of primary instability and vice versa.

Now if there was a whole hierarchy of instabilities which occurred and which for a short time could be distinguished by scale, the higher order instabilities would help the growth rate of the lower orders, and the other way around. We may guess that the larger the number of higher order instabilities that can participate, the more violent the growth rate, the higher the production of turbulence and the quicker the large scale flow will be drained of available vorticity. Thus, for high Reynolds numbers, the bursts of turbulence production should be expected to be more intense but shorter in duration.

Evidence for intermittent three-dimensional instability has been obtained by Kline and his associates, and more recently by Gupta, Laufer and Kaplan.[11] Figure 19 shows an example of spanwise velocity correlations which were found by short-time averaging of velocity fluctuations.

VI.3 Pressure Field due to a Burst of Turbulence Production

Taking the divergence of the momentum equation, ignoring viscous stresses, one obtains

$$\partial/\partial x_j[\partial Q_i/\partial t + \partial(Q_iQ_j)/\partial x_j] = -\nabla^2\Pi/\rho \qquad (6.2)$$

or, taking account of the continuity equation for incompressible flow:

$$\nabla^2\Pi/\rho = -\partial^2(Q_iQ_j)/\partial x_i\partial x_j \qquad (6.3)$$

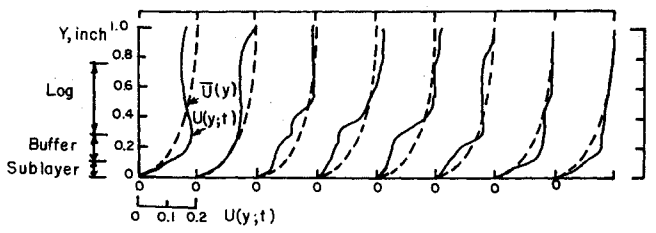

Fig. 18 Sequence of velocity profiles during a burst of production (from Ref. 12).

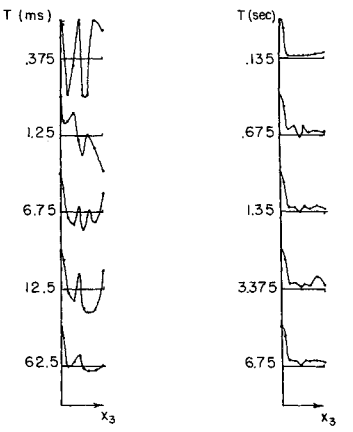

Fig. 19 Spanwise space correlations of streamwise velocity in sublayer as function of averaging time T, showing how fine structure is wiped out by longer time averaging (from Ref. 17).

Substituting for $Q_i = U_i + \mathfrak{U}_i + u_i$ and similarly for pressure, one finds, after averaging over a scale larger than the scale of $\mathfrak{U}$ but smaller than the burst:

$$\nabla^2\bar{\mathcal{P}} = -\rho(\partial^2/\partial x_i\partial x_j)\{(\mathfrak{U}_i\mathfrak{U}_j + \langle u_iu_j\rangle)\} \qquad (6.4)$$

having assumed that the large scale motion can be ignored here as being independently in equilibrium or too slowly varying to contribute much to either side of the equation. Thus, there is a pressure field associated with a turbulence production event, that is a Reynolds stress burst, and the scale of the pressure pattern is the scale of the bursts, not the scale of the local fluctuations within the burst. Therefore, we must expect the fluid within the burst to be accelerated; this may contain an explanation of the violent ejection of turbulent fluid away from the sublayer as observed by Kline and shown in Fig. 18, as a movement upwards of the free shear layer portion of the velocity profile.

In the spanwise center surface of a patch of production, the dominant term on the right of Eq. (6.4) will most likely be:

$$\partial^2/\partial x_1\partial x_2\{(\mathfrak{U}_1\mathfrak{U}_2 + \langle u_1u_2\rangle)\}$$

and one should guess that $(\{\mathfrak{U}_1\mathfrak{U}_2\} + \{\langle u_1u_2\rangle\})$ is predominantly an even function of x_1, as measured streamwise from the middle of the patch. This means that the derivative is odd in x_1 and therefore is an odd function of x_1 distance from the center of the patch. The vertical velocity of fluid within the patch is upward as the patch reacts to the pressure field it generates. This may furnish a partial explanation of the results of the pressure—velocity correlation measurements of Willmarth,[18] as shown in Fig. 20, as the contour of the instantaneous correlation between wall pressure at $(X_1, 0, 0)$ and spanwise velocity $u_3 = w\,(x_1 + \xi, x_2, x_3)$ for four values of ξ.

One can see the surface of zero correlation lift with downstream distance, and may imagine that the sets of closed contours may be associated with vortices.

VI.4 Large Scale Eddies

Landahl[19] has shown that the wall pressure space-time correlation in a turbulent boundary layer can be approximated by considering the wall pressure fluctuations being due to the characteristic modes of the mean profile and excited by white noise.

He takes the mean velocity profile, performs a linear stability analysis to find the propagation characteristics of disturbances as function of frequency. These disturbances are all damped, since the mean velocity profile of the flow is stable. He then assumes that the excitation is white noise, computes the corresponding properties of the wall pressure correlations and finds reasonable agreement with experiments for convection velocity and streamwise decay of cross-spec-

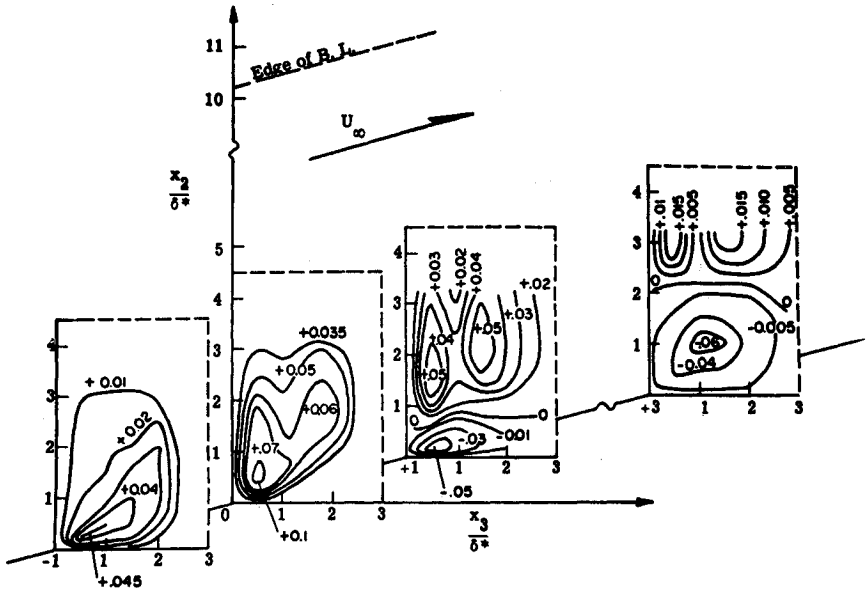

Fig. 20 Contours of constant correlation between wall pressure at $(x,0,0)$ and spanwise velocity at $(x_1 + \xi, x_2, x_3)$ for four values of ξ (from Ref. 18).

tral density. Figure 21 shows how his results compare with observations of Willmarth and Woolridge.[20]

If indeed the production events are intermittent and short, the spectral characteristics of the associated stress patterns should be similar to white noise at least for low frequencies. Thus, a possible explanation of the success of linear analysis, as demonstrated by Landahl, may be that the large scale disturbances may indeed be created by generating events, but that their subsequent development is largely independent of bursts of generation, the latter being relatively rare.

VI.5 Recapitulation

Based on the experimental results available so far, it appears that the bursts of turbulence generation may be started by accidental distortions of the velocity profile due to large eddies interacting. These larger scale disturbances were produced upstream by other production events.

The production event involves strong interactions between many scales of motion, and the growth rate of disturbances may greatly exceed that predicted by linear theory. The production patches are finite in scale, move, and represent transient stress anomalies of a scale equal to the size of the patch.

The event terminates in a violent ejection of fluid away from the wall, caused by interaction of the pressure pattern generated by the burst with the large scale velocity field and the excitation of a large scale wave. For increasing Reynolds numbers, the production events become more violent and more intermittent.

In order to throw some additional light on these processes, we shall next show some examples of how modifications of the fluid or the boundary conditions change the processes.

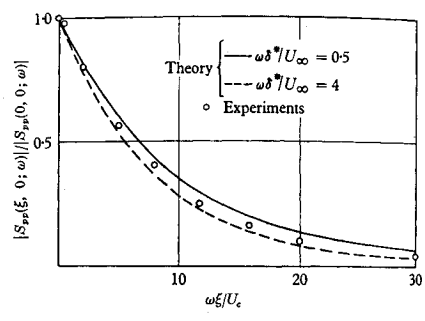

Fig. 21 Streamwise decay of crosspectral density of wall pressure (from Ref. 19).

VII. Examples of Effects of Changes in Fluid or Boundary Conditions

To start with one extreme example, we look at some data from the boundary layer over the sea surface, obtained by Barger[21] et al. The Reynolds numbers for these measurements, based on an upstream distance of the seabreeze field of 50 km and a wind of 20 knots is 5×10^{11}. The estimated momentum thickness Reynolds number is 10^8, thus well beyond what can be achieved in wind-tunnel experiments. The intermittency of turbulent fluctuations are shown in Fig. 17. The production of turbulence for this case must involve the dynamics of the boundary, which is capable of supporting surface waves of scales covering a range from 10^{-1} cm to 10^5 cm at least. The work done on the water to make waves must equal a stress times a strain, thus, the reactions of the stresses on the water act on the air to produce turbulence.

Figure 22 shows the amplitude of selected bands of surface waves vs time. The patchiness of occurrence of small scale disturbances and their phase relationship to the big waves is apparent.

We changed the dynamics of the surface by covering it by a $\frac{1}{2}$km^2 slick of oleyl alcohol, effectively eliminating the capillary waves. The striking effect on the large scale wave field is shown in Fig. 23, which shows the wave spectrum before A, during B and after C the slickpassage. The presence of small scale unstable disturbances obviously has a profound effect upon the generation of large scale disturbances of scales 10^4 larger. Barger[21] et al. also have shown a strong effect of slicks on the correlation between sea-surface slope and air velocity fluctuations.

Yet another example is the effect of the addition of long chain polymers to water upon a turbulent pipe flow. Virk,[22] among others, has shown the effect of such additives upon skin friction, and has offered as an explanation the role of the molecules as mechanisms for energy storage in extensional vibrations. This role can at least be made plausible by looking at the energy equations, interpreting the velocity fields differently.

Say that: U_i is the mean flow; $\mathfrak{U}_i$ is the turbulent velocity field; and u_i is a velocity field which is coupled to molecular vibration. Even if u_i is of much smaller time and space scales than $\mathfrak{U}_i$, Eq. (4.9) shows that $\langle e \rangle$ may be excited preferentially at certain phases of $\mathfrak{U}_i$, where $\partial\mathfrak{U}_i/\partial x_j$ is large, as long as an instability is possible. Be that as it may, Eq. (4.8) shows that if $\langle u_i u_j \rangle$ occurs preferentially at certain phases of $\mathfrak{U}_i$, the production of $\mathfrak{U}_i$ is affected. Thus, it is not the scale of the fluctuations of the small scales, but the size

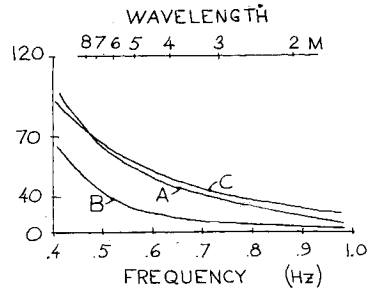

Fig. 22 Wave gage output in selected frequency bands, showing intermittent occurrence of high-frequency waves.

of the region of fluctuation which matters. These examples illustrate how fluctuations of great disparity in scale may strongly interact, and we shall mention a few more examples of disparate scale interactions.

VIII. Examples of Strong Interactions between Disparate Scales of Motion

One familiar example of a flow where instabilities of very different scales occur is the flow of a jet from a short orifice, where the boundary-layer thickness at the exit is much smaller than the jet diameter. The thin free shear layer will be unstable with wavelengths of fluctuation proportional to shear layer thickness. This shear layer instability is rather orderly, although the growth of fluctuations is rapid.

If this flow is coupled to the instability of the jet as a whole, one may speculate that the production events of shear layer turbulence may take place at preferred phases of the large scale oscillations. These patches of production may be rather well organized, be much larger then the shear layer thickness, and certainly be well defined geometrically. The pressure field associated with such patches is given by Eq. (6.4):

$$\nabla^2\bar{\mathcal{P}} = -\rho(\partial^2/\partial x_i\partial x_j)(\{\mathcal{U}_i\mathcal{U}_j\} + \{\langle u_iu_j\rangle\}) \qquad (6.4)$$

to an inviscid, incompressible approximation, and the right-hand side is Lighthill's[23] source term for aerodynamic sound. One may therefore speculate that at very high Reynolds number, where there is room for great disparity in scales of turbulence, these patches may act as strongly directional intermittent emitters of sound. The crackling noise one hears in certain directions from large jets may be caused by this phenomenon, although more research is needed to discover the exact mechanism.

Yet another example of very large Reynolds number phenomena where turbulence is patchy, is found in the atmosphere, where patches of turbulence of a large range of scales are surrounded by quiescent regions. Fronts, squalls and clear air turbulence regions are examples. This brings up the difficulty of describing such phenomena in terms of time average statistical measures, which is where we started.

IX. Observation of Intermittent Events

Intermittent events tend to get lost in time-averages, unless one only measures variables which are uniquely typical of the events. Reynolds stress may be such a unique variable for very high Reynolds number turbulent flow. If one can find an indicator of an event, one may then measure other variables intensively for the duration of the event. Such conditional sampling techniques have been used by Kovasznay and by others. A crude statement of the idea is that if events are similar, one should measure the living daylights out of one and then sit back and count to get the average effect.

In order to illuminate the dynamics of intermittent production of turbulence, we must attempt to devise experiments

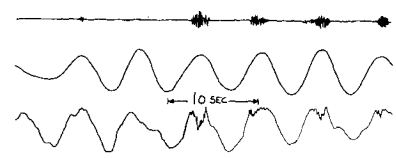

Fig. 23 Spectra of sea surface waves before (A), during (B) and after (C) the passage of a $\frac{1}{2}$ km² surface slick (from Ref. 21).

that pose intelligent questions of nature, so to say. Examples of such questions are:

How does production burst duration and frequency of occurrence vary with Reynolds number for a given flow?

If we choose a frequency ω_0 or wavenumber k_0, how do Reynolds stresses due to fluctuations of all higher frequencies or wavenumbers correlate to the fluctuations of lower frequencies or wavenumbers? How does this correlation vary with ω_0 or k_0? This, in effect, attempts to resolve the term

$$\langle u_iu_j\rangle\partial\mathcal{U}_i/\partial x_j$$

in the frequency domain. What is the space-time correlation between pressure and Reynolds stress? How can this be resolved in the frequency domain?

What is the structure of a burst of production and can one describe its time development? This is in fact what the measurements of Gupta[17] and of Kim and Kline suggest.

One may next ask whether the growth rate of a disturbance $\mathcal{U}$ due to stresses from smaller scale bursts should not be a function of $\mathcal{U}$. If this effect is dominating, one may expect a logarithmic-normal distribution in energy of larger scale disturbances. What is the probability distribution function of the energy in spectral components?

These questions, of course, make one envision complicated arrays of hot wires and transducers, so complicated in fact, that one wishes one were smart enough to avoid such complexity. To discover such experiments is of course the challenge for the future.

However, all experiments on turbulence and turbulent production at high Reynolds number will have to employ some kind of conditional sampling to avoid having the averaging over adolescence and death of turbulence obscure the dynamics of generation.

X. Conclusion

I have attempted to illustrate where we now are in our understanding of turbulent flow as seen from an experimenter's viewpoint. Although the arguments may be crude and incomplete, I hope some of the dynamics of turbulence may have been communicated, and that I have not irritated the experts too much in the process.

References

[1] Tollmien, W., "Über die Entstehung der Turbulenz," *Mathematisch-Naturwissenschaftliche Klassennachrichten*, Gesellschaft der Wissenschaften, Göttingen, 1929, pp. 21–44.

[2] Schlichting, H., "Über die Entstehung der Turbulenz bei der Plattenströmung," *Mathematisch-Naturwissenschaftliche Klassennachrichten*, Gesellschaft der Wissenschaften, Göttingen, 1932, pp. 160–198.

[3] Lin, C. C., *The Theory of Hydrodynamic Stability*, Cambridge University Press, London, 1955.

[4] Benney, D. C. and Lin, C. C., "On the Secondary Motions Induced by Oscillations in Shear Flow," *The Physics of Fluids*, Vol. 3, 1960, pp. 656–657.

[5] Schubauer, G. B. and Klebanoff, P. S., "Contributions on the Mechanics of Boundary Layer Transition," Rept. 1289, 1956, NACA.

[6] Klebanoff, P. S., Tidstrom, K. D., and Sargent, L. M., "The Three-Dimensional Nature of Boundary Layer Instability," *Journal of Fluid Mechanics*, Vol. 12, 1962, pp. 1–34.

[7] Greenspan, H. P. and Benney, D. J., "On Shear Layer Instability, Breakdown and Transition," *Journal of Fluid Mechanics*, Vol. 15, 1963, p. 133.

[8] Emmons, H. W., "The Laminar-Turbulent Transition in a Boundary Layer," Pt. I, *Journal of Atmospheric Sciences*, Vol. 18, 1958, p. 490.

[9] Starr, V. P., *"Physics of Negative Viscosity Phenomena,"* McGraw-Hill, New York, 1968.

[10] Squire, H. B., "On the Stability of Three-Dimensional Disturbances of Viscous Flow between Parallel Walls," *Proceedings of the Royal Society*, Vol. A 142, 1933, p. 621.

[11] Kovasznay, L. S. G., "Detailed Flow Field in Transition," *Proceedings of the 1962 Heat Transfer and Fluid Mechanics Conference*, Stanford University Press, 1962.

[12] Kim, H. T., Kline, S. J., and Reynolds, W. C., "An Experimental Study of Turbulence Production near a Smooth Wall in a Turbulent Boundary Layer with Zero Pressure Gradient," Rept. MD 20, 1968, Dept. of Engineering, Stanford Univ., Calif.

[13] Coles, D., "The Law of the Wake and the Turbulent Boundary Layer," *Journal of Fluid Mechanics*, Vol. 1, 1956, p. 191.

[14] Klebanoff, P. S., "Characteristics of Turbulence in a Boundary Layer with Zero Pressure Gradient," Rept. 1247, 1955, NACA.

[15] Laufer, J., "The Structure of Fully Developed Pipe Flow," Rept. 1174, 1954, NACA.

[16] Grant, H. L., Stewart, R. W., and Moilliet, A., "Turbulence Spectra from a Tidal Channel," *Journal of Fluid Mechanics*, Vol. 12, 1962, p. 241.

[17] Gupta, A. K., "An Experimental Investigation of the Viscous Sublayer Region in a Turbulent Boundary Layer," Ph.D. thesis, 1970, Univ. of Southern California.

[18] Willmarth, W. W. and Bo Jang Tu., "Structure of Turbulence in the Boundary Layer near the Wall," *The Physics of Fluids*, Supplement 10, 1967, p. 134.

[19] Landahl, M. T., "A Wave-Guide Model for Turbulent Shear Flow," *Journal of Fluid Mechanics*, Vol. 29, 1967, p. 331.

[20] Willmarth, W. W. and Woolridge, C. E., "Measurement of the fluctuating pressure at the wall beneath a thick boundary layer," *Journal of Fluid Mechanics*, Vol. 11, 1962, p. 187.

[21] Barger, W. R., Garrett, W. D., Mollo-Christensen, E. L., and Ruggles, K. W., "Effects of an Artificial Sea Slick upon the Atmosphere and the Ocean," *Journal of Applied Meteorology*, Vol. 9, 1970, pp. 396–400.

[22] Virk, P., "An Elastic Sublayer Model for Drag Reduction by Dilute Solutions of Linear Micromoleculae," to be published in the *Journal of Fluid Mechanics*, 1970.

[23] Lighthill, J. M., "On Sound Generated Aerodynamically," Pt. II, *Proceedings of the Royal Society*, Vol. A 222, 1954, p. 1.

JULY 1971 AIAA JOURNAL VOL. 9, NO. 7

Reduction of Launch Vehicle Injection Errors by Trajectory Shaping

RICHARD ROSENBAUM*
Lockheed Missiles & Space Company, Palo Alto, Calif.

A method is presented for shaping a booster trajectory to minimize the sensitivity of terminal constraints to variations in vehicle or atmosphere parameters. The unique feature of the problem is that the payoff function depends not only on the state variables and the controls, but also on the adjoint variables (Lagrange multipliers). In order to apply the gradient optimization technique, two new sets of differential equations must be integrated. An example, using the Scout booster, is given in which it is shown that the sensitivity of terminal altitude to variations in first stage burn rate can be reduced by 50%.

Nomenclature

f = vector of derivatives of state variables
P = vector of system variables
q = vector of system parameters
t = time
T = thrust
x = vector of state variables
α = vector of control variables
θ = thrust attitude angle
λ = vector of adjoint variables associated with the altitude constraint
λ_ψ = vector of adjoint variables associated with constraint ψ
Λ_P = influence coefficient relating P to ψ
Λ_φ = influence coefficient relating α to φ
μ = vector of adjoint variables associated with λ_ψ
ν = vector of adjoint variables associated with the sensitivity payoff
ξ = vector of control parameters
φ = sensitivity payoff

Superscripts

f = final
i = initial
T = transpose

Subscripts

n = nominal
p = perturbed

Presented as Paper 70-1078 at the AAS/AIAA Astrodynamics Conference, Santa Barbara, Calif., August 19–21, 1970; submitted September 15, 1970; revision received January 29, 1971. This work was supported by the Langley Research Center under Contract NAS 1-8920. The author would like to thank J. V. Breakwell of Stanford University for several illuminating discussions and R. E. Willwerth for assistance in performing the study. Z. Taulbee was responsible for the computer programing.

* Research Scientist, Mathematics and Operations Research Laboratory. Member AIAA.

Introduction

THE advent of the high-speed digital computer, together with the development of the gradient method of trajectory optimization, has made it possible to rapidly determine the maximum performance of booster vehicles. In many cases, however, the capability of the booster exceeds the mission requirements. The payload to be placed in orbit, for example, may weigh considerably less than the maximum payload that the booster can deliver into orbit. A variety of trajectories will satisfy the mission requirement. It is